Journal of Organometallic Chemistry, 466 (1994) 211–220

Ruthenium carbonyl cluster complexes with nitrogen ligands III *. Reaction of $Ru_3(\mu\text{-}AuPPh_3)(\mu\text{-}Cl)(CO)_{10}$ with pyridine; crystal structures of $Ru_3(\mu\text{-}H)(\mu\text{-}NC_5H_4)(CO)_9(PPh_3)$, $Ru_3(\mu\text{-}Cl)_2(CO)_8(NC_5H_5)(PPh_3)$ and $Ru_3(\mu\text{-}Cl)_2(CO)_8(NC_5H_5)_2$

Marie P. Cifuentes and Mark G. Humphrey

Department of Chemistry, University of New England, Armidale, N.S.W. 2351 (Australia)

Brian W. Skelton and Allan H. White

Department of Chemistry, University of Western Australia, Nedlands, W.A. 6009 (Australia)

(Received May 19, 1993)

Abstract

The reaction between $Ru_3(\mu\text{-}AuPPh_3)(\mu\text{-}Cl)(CO)_{10}$ (1) and pyridine afforded a mixture of products from which the title complexes $Ru_3(\mu\text{-}H)(\mu\text{-}NC_5H_4)(CO)_9(PPh_3)$ (4), $Ru_3(\mu\text{-}Cl)_2(CO)_8(NC_5H_5)(PPh_3)$ (6) and $Ru_3(\mu\text{-}Cl)_2(CO)_8(NC_5H_5)_2$ (7) have been obtained together with the previously reported pyridyl cluster $Ru_3(\mu\text{-}H)(\mu\text{-}NC_5H_4)(CO)_{10}$ (2) and the phosphine-substituted clusters $Ru_3(CO)_{10}(PPh_3)_2$ (3) and $Ru_3(\mu\text{-}Cl)_2(CO)_8(PPh_3)_2$ (5). Complex 4 has also been obtained with a high yield by phosphine substitution of 2 under mild conditions. The structural study of 4 reveals site-specific substitution at the N-ligated ruthenium. Products 5–7 are dichloro-bridged complexes related by successive replacement of PPh_3 by NC_5H_5. Single-crystal X-ray diffraction studies of 6 and 7 indicate that these complexes contain triruthenium cores incorporating one and two σ-bound equatorially disposed pyridine ligands respectively, a new coordination mode for unsupported pyridine ligands on triruthenium clusters. Extremely long Ru–N distances in 6 and 7 are consistent with the "lightly stabilizing" nature of the pyridine ligand in trinuclear cluster chemistry. A comparison of the core geometries of 5–7 has revealed a contraction in the Ru–Ru distances on sequential replacement of the *P*-donor ligand by the *N*-donor ligand.

Key words: Ruthenium; Carbonyl; Pyridine; Crystal structure

1. Introduction

The reactions of ruthenium clusters with nitrogen ligands are of much current interest and have been recently reviewed [2]. A suitable choice of nitrogen-donor molecule with a ruthenium cluster can serve to model the heterogeneously catalysed hydrodenitrogenation process. Pyridine and its higher homologues are believed to be the most persistent N-containing impurities in liquid fuels [3], and we have recently reported the reactions of $Ru_3(CO)_{12}$ with pyridine [4] and piperidine [1]; the latter is a likely reduction intermediate of pyridine. Hydrodenitrogenation must, of necessity, involve N–C bond cleavage at some stage. N–C weakening is a necessary step in N–C cleavage, and our studies with piperidine have shown that multimetal coordination of the N-ligand leads to substantial N–C bond weakening compared with bimetal coordination. We therefore decided to seek multimetal coordination of pyridine. One possible route to this involves the addition of another metal to the triruthenium core, and so we have examined precursors to mixed-metal clusters incorporating ruthenium and pyridine or pyridyl ligands and report below our first forays into the field, with gold as the heterometal.

2. Results and discussion

Reaction of the preformed aurotriruthenium cluster $Ru_3(\mu\text{-}AuPPh_3)(\mu\text{-}Cl)(CO)_{10}$ (1) [5] with an excess of

Correspondence to: Dr. M.G. Humphrey.

* For Part II, see ref. 1.

0022-328X/94/$7.00
SSDI 0022-328X(93)23970-9

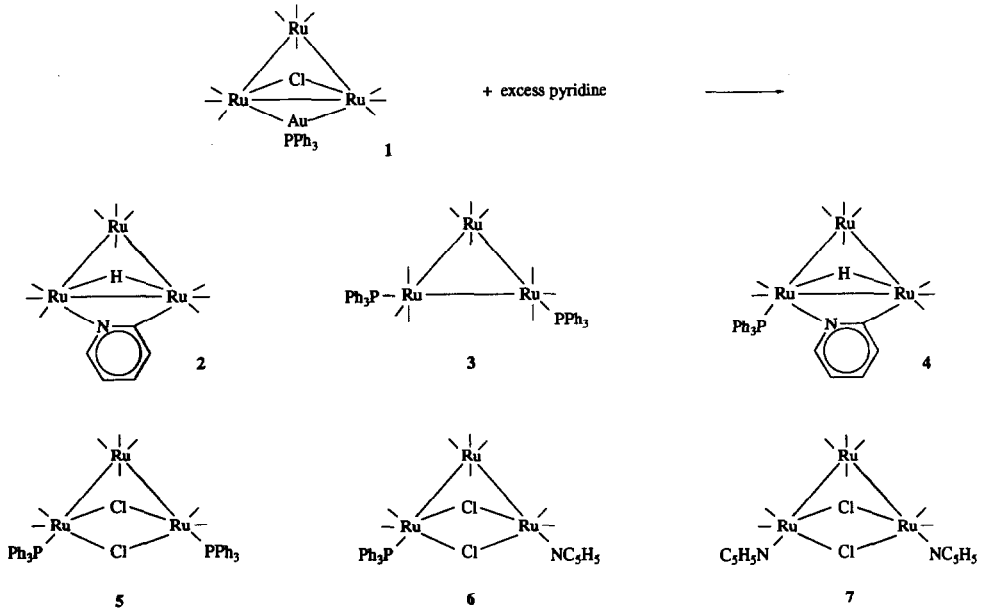

Scheme 1.

pyridine in refluxing tetrahydrofuran (THF) afforded a mixture of at least eight products, of which six were identified after thin layer chromatography. Band 1, the fastest moving band, was crystallized and identified as $Ru_3(\mu\text{-}H)(\mu\text{-}NC_5H_4)(CO)_{10}$ (**2**), which we have previously obtained with a high yield from direct reaction between $Ru_3(CO)_{12}$ and pyridine [4]. Band 2 was crystallized and identified as $Ru_3(CO)_{10}(PPh_3)_2$ (**3**) [6]. This bis(phosphine) triruthenium cluster was previously obtained from reaction between $Ru_3(CO)_{12}$ and PPh_3 in hexane, a solvent in which it is sparingly soluble; in more polar solvents, further reaction to afford

TABLE 1. Summary of crystallographic data for $Ru_3(\mu\text{-}H)(\mu\text{-}NC_5H_4)(CO)_9(PPh_3)$ (**4**), $Ru_3(\mu\text{-}Cl)_2(CO)_8(NC_5H_5)(PPh_3)$ (**6**) and $Ru_3(\mu\text{-}Cl)_2(CO)_8(NC_5H_5)_2$ (**7**)

	4	**6**	**7**
Formula	$C_{32}H_{20}NO_9PRu_3$	$C_{31}H_{20}Cl_2NO_8PRu_3$	$C_{18}H_{10}Cl_2N_2O_8Ru_3$
M	896.7	939.6	756.4
Crystal system	Monoclinic	Triclinic	Monoclinic
Space group	$P2_1/c$ (No.14)	$P\bar{1}$ (No.2)	$P2_1/c$
a (Å)	9.367(4)	17.644(4)	12.829(8)
b (Å)	24.013(8)	11.025(6)	26.339(8)
c (Å)	16.896(4)	9.336(3)	16.009(10)
α (°)		71.70(3)	
β (°)	120.60(4)	89.36(2)	119.46(5)
γ (°)		87.01(3)	
V (Å^3)	3270	1722	4710
Z	4	2	8
$D_{calc.}$ (g cm^{-3})	1.82	1.81	2.13
μ_{Mo} (cm^{-1})	13.4	15.2	19.7
Specimen (mm × mm × mm)	0.35 × 0.30 × 0.20	0.06 × 0.32 × 0.09	0.14 × 0.09 × 0.18
A^* minimum; A^* maximum	1.10, 1.19	1.06, 1.13	1.18, 1.26
$F(000)$	1752	916	2896
$2\theta_{max}$ (°)	50	46	50
N	5730	4734	7801
N_o	3676	3467	4479
R	0.039	0.046	0.046
R_w	0.038	0.052	0.045

$Ru_3(CO)_9(PPh_3)_3$ occurs. The formation of both **2** and **3** strongly suggests the intermediacy of a coordinatively unsaturated "$Ru_3(CO)_{10}$" species by elimination of (phosphine)gold and chloro moieties; indeed, the "lightly stabilized" $Ru_3(CO)_{10}(MeCN)_2$ reacts with both pyridine and PPh_3, to afford **2** and **3** [7], respectively (Scheme 1).

Bands 3 and 5 were minor and their content not identified. The product from band 4 was crystallized and identified as $Ru_3(\mu\text{-}H)(\mu\text{-}NC_5H_4)(CO)_9(PPh_3)$ (**4**) by a combination of IR, ^1H and ^{13}C nuclear magnetic resonance (NMR), fast atom bombardment (FAB), mass spectrometry (MS) and microanalysis. The FAB mass spectrum contains no molecular ion, instead showing an ion corresponding to $[M-CO]^+$ at the highest m/z value. The ^1H NMR spectrum contains

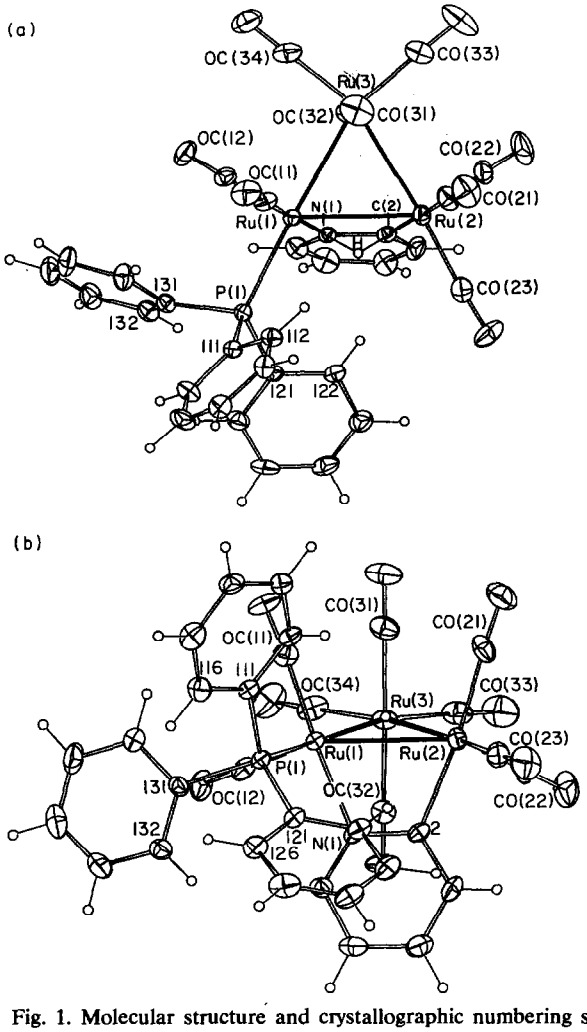

Fig. 1. Molecular structure and crystallographic numbering scheme for $Ru_3(\mu\text{-}H)(\mu\text{-}NC_5H_4)(CO)_9(PPh_3)$ (**4**); 20% thermal ellipsoids are shown for the non-hydrogen atoms. Hydrogen atoms have arbitrary radii of 0.1 Å. Projections are shown (a) normal to and (b) oblique to the Ru_3 plane.

TABLE 2. Atomic coordinates and equivalent isotropic thermal parameters for $Ru_3(\mu\text{-}H)(\mu\text{-}NC_5H_4)(CO)_9(PPh_3)$ (**4**)

Atom	x	y	z	U_{eq} (Å^2)
Ru(1)	0.41373 (7)	0.60563 (2)	0.80569 (4)	0.0347 (3)
Ru(2)	0.47795 (8)	0.57636 (2)	0.65916 (4)	0.0439 (3)
Ru(3)	0.32471 (8)	0.49871 (2)	0.72171 (4)	0.0472 (3)
C(11)	0.188 (1)	0.6232 (3)	0.7516 (5)	0.054 (4)
O(11)	0.0534 (7)	0.6350 (3)	0.7236 (5)	0.079 (4)
C(12)	0.4158 (9)	0.5744 (3)	0.9083 (6)	0.054 (5)
O(12)	0.4159 (8)	0.5561 (2)	0.9697 (4)	0.074 (4)
C(21)	0.270 (1)	0.5829 (3)	0.5432 (6)	0.067 (5)
O(21)	0.1537 (9)	0.5884 (3)	0.4735 (4)	0.099 (4)
C(22)	0.554 (1)	0.5143 (3)	0.6237 (6)	0.066 (5)
O(22)	0.608 (1)	0.4782 (3)	0.6030 (5)	0.107 (5)
O(23)	0.6480 (9)	0.6618 (3)	0.6030 (5)	0.099 (5)
C(23)	0.585 (1)	0.6301 (4)	0.6263 (6)	0.064 (5)
C(31)	0.115 (1)	0.5308 (3)	0.6307 (6)	0.066 (5)
O(31)	−0.0123 (8)	0.5465 (3)	0.5772 (5)	0.101 (4)
C(32)	0.545 (1)	0.4759 (3)	0.8149 (5)	0.050 (4)
O(32)	0.6695 (7)	0.4586 (3)	0.8686 (4)	0.079 (3)
C(33)	0.310 (1)	0.4383 (4)	0.6460 (7)	0.074 (5)
O(33)	0.308 (1)	0.4011 (3)	0.6020 (6)	0.125 (5)
C(34)	0.227 (1)	0.4687 (4)	0.7886 (7)	0.070 (5)
O(34)	0.1666 (9)	0.4515 (3)	0.8273 (5)	0.101 (5)
P(1)	0.4913 (2)	0.69630 (7)	0.8706 (1)	0.0368 (9)
C(111)	0.3465 (8)	0.7532 (3)	0.8110 (5)	0.039 (4)
C(112)	0.2358 (9)	0.7499 (3)	0.7176 (5)	0.046 (4)
C(113)	0.1288 (9)	0.7945 (3)	0.6720 (5)	0.055 (4)
C(114)	0.132 (1)	0.8407 (3)	0.7191 (6)	0.058 (5)
C(115)	0.241 (1)	0.8443 (3)	0.8103 (7)	0.068 (6)
C(116)	0.349 (1)	0.8016 (3)	0.8574 (5)	0.057 (4)
C(121)	0.6865 (8)	0.7271 (3)	0.8910 (5)	0.040 (4)
C(122)	0.7462 (9)	0.7110 (3)	0.8353 (5)	0.046 (4)
C(123)	0.887 (1)	0.7360 (4)	0.8437 (7)	0.067 (5)
C(124)	0.967 (1)	0.7757 (4)	0.9085 (7)	0.067 (5)
C(125)	0.909 (1)	0.7931 (3)	0.9532 (6)	0.066 (5)
C(126)	0.7684 (9)	0.7685 (3)	0.9661 (6)	0.056 (4)
C(131)	0.5059 (9)	0.6960 (3)	0.9824 (5)	0.043 (3)
C(132)	0.6531 (9)	0.6871 (3)	1.0643 (5)	0.051 (4)
C(133)	0.653 (1)	0.6803 (4)	1.1447 (6)	0.073 (5)
C(134)	0.508 (2)	0.6805 (4)	1.1454 (7)	0.086 (7)
C(135)	0.361 (1)	0.6882 (4)	1.0651 (7)	0.083 (6)
C(136)	0.359 (1)	0.6957 (4)	0.9845 (6)	0.063 (5)
N(1)	0.6645 (7)	0.5855 (2)	0.8578 (4)	0.035 (3)
C(2)	0.6928 (8)	0.5724 (3)	0.7905 (5)	0.039 (4)
C(3)	0.858 (1)	0.5609 (3)	0.8146 (6)	0.061 (5)
C(4)	0.982 (1)	0.5622 (4)	0.9036 (7)	0.068 (5)
C(5)	0.949 (1)	0.5735 (4)	0.9703 (6)	0.067 (5)
C(6)	0.788 (1)	0.5863 (3)	0.9455 (5)	0.051 (4)
H	0.415 (8)	0.632 (3)	0.706 (4)	0.07 (2)

signals at 7.45–7.31 (m, 16H) ppm attributable to the phenyl groups of the triphenylphosphine ligand and the H6 of the pyridyl ligand. Signals at 7.25 (m, 1H), 7.00 (m, 1H) and 6.24 (m, 1H) ppm can be assigned to the H3, H4 and H5 respectively of the pyridyl moiety. A characteristic hydrido resonance appears as a doublet ($J_{HP} = 9$ Hz) at −14.08 ppm; the coupling constant is indicative of *cis*-coordinated hydrido and phosphine ligands (*cis* coupling has been observed in the

TABLE 3. Selected bond lengths and angles for $Ru_3(\mu\text{-H})(\mu\text{-}NC_5H_4)(CO)_9(PPh_3)$ (4)

Distances			
Ru(1)–Ru(2)	2.916 (1)	Ru(2)–H	1.80 (8)
Ru(1)–Ru(3)	2.845 (1)	N(1)–C(2)	1.33 (1)
Ru(2)–Ru(3)	2.863 (1)	N(1)–C(6)	1.339 (8)
Ru(1)–P(1)	2.379 (2)	C(2)–C(3)	1.41 (1)
Ru(1)–N(1)	2.103 (6)	C(3)–C(4)	1.36 (1)
Ru(1)–H	1.80 (8)	C(4)–C(5)	1.34 (2)
Ru(2)–C(2)	2.106 (6)	C(5)–C(6)	1.37 (1)
Angles			
Ru(1)–H–Ru(2)	108 (3)	Ru(3)–Ru(2)–C(2)	88.3 (2)
Ru(2)–Ru(1)–Ru(3)	59.59 (3)	Ru(3)–Ru(2)–H	89 (3)
Ru(2)–Ru(1)–P(1)	117.76 (7)	C(2)–Ru(2)–H	85 (2)
Ru(2)–Ru(1)–N(1)	68.3 (2)	Ru(1)–Ru(3)–Ru(2)	61.43 (3)
Ru(2)–Ru(1)–H	36 (2)	Ru(1)–N(1)–C(2)	111.3 (4)
Ru(3)–Ru(1)–P(1)	177.33 (7)	Ru(1)–N(1)–C(6)	127.8 (6)
Ru(3)–Ru(1)–N(1)	89.0 (1)	C(2)–N(1)–C(6)	120.8 (7)
Ru(3)–Ru(1)–H	89 (2)	Ru(2)–C(2)–N(1)	113.0 (5)
P(1)–Ru(1)–N(1)	90.2 (1)	Ru(2)–C(2)–C(3)	129.2 (7)
P(1)–Ru(1)–H	88 (2)	N(1)–C(2)–C(3)	117.7 (6)
N(1)–Ru(1)–H	86 (2)	C(2)–C(3)–C(4)	121 (1)
Ru(1)–Ru(2)–Ru(3)	58.98 (3)	C(3)–C(4)–C(5)	119.7 (9)
Ru(1)–Ru(2)–C(2)	67.4(3)	C(4)–C(5)–C(6)	118.5 (7)
Ru(1)–Ru(2)–H	36 (2)	N(1)–C(6)–C(5)	122.1 (9)

range 5–10 Hz, and *trans* coupling between 23 and 30 Hz) [8]. As further confirmation of the identity of **4**, the direct reaction between **2** and PPh_3 in THF was investigated; **4** was obtained as the site-specific substitution product with a 81% yield. Given this result, it is highly likely that **4** originates from reaction intermediates **2** and PPh_3 in the aurotriruthenium cluster-pyridine system; PPh_3 is cleaved from gold readily. It was not possible to assign a coordination site definitively to the phosphine ligand (based on the spectroscopic data, both the C(pyridyl)- and N-ligated rutheniums are possible phosphine sites), so a single-crystal X-ray structural study was performed on **4**.

The solid state structure of **4** is shown in Fig. 1; crystallographic data are listed in Table 1, atomic coordinates in Table 2, and selected bond lengths and angles in Table 3. The three metal atoms form a triangle with the pyridyl and a hydrido ligand bridging the longest Ru–Ru bond; a marginal lengthening of the ligand-bridged bond in similar structures with (μ-H) and (μ-RN=CR) was noted previously [1].

The hydride was located, with the Ru_2H dihedral angle at 48(4)° to the plane of the ruthenium triangle, and symmetrically disposed (Ru–H, 1.80(8) Å); located hydrido ligands are rare in structures of this type [1]. The Ru_2NC unit was found to be at 77.7(2)° to the Ru_3 plane. The Ru(1)–N(1) distance (2.103(6) Å) and Ru(2)–C(2) distance (2.106(6) Å) are not significantly different, in contrast with our tabulated data for related structures, in which Ru–N bonds were found to be shorter than Ru–C bonds. Distances within the axially- coordinated pyridyl ligand (average C–C, 1.37 Å; average C–N, 1.34 Å) and lack of "bond alternation" are consistent with preservation of the aromaticity of the pyridine on coordination; in particular, the coordinated C–N (1.33(1) Å) is not significantly different from the free C–N of the ligand (1.339(8) Å), and substantially longer than C–N distances in related triruthenium clusters with non-aromatic μ-η^2-RN=CR′ ligands (average, 1.27 Å) [1]. Pyridyl-ligated ruthenium–carbonyl distances are all 1.88(1) Å except for *trans* to the metallated pyridyl carbon atom, which is substantially longer at 1.94(1) Å; the average Ru–CO for the non-pyridyl-ligated ruthenium atom is 1.92 Å. Ru–C–O angles (average, 177°) are unexceptional.

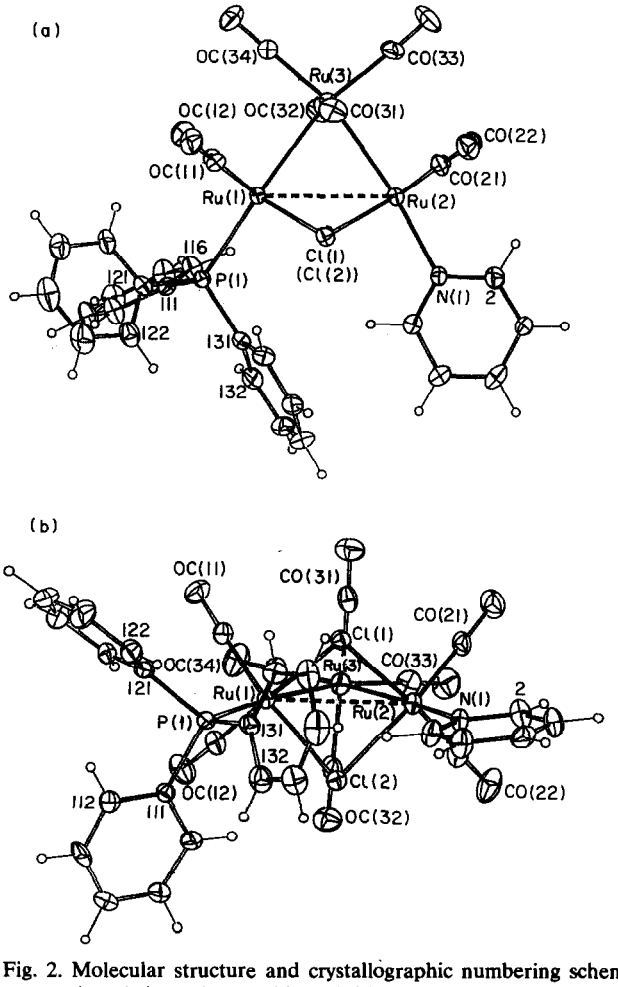

Fig. 2. Molecular structure and crystallographic numbering scheme for $Ru_3(\mu\text{-}Cl)_2(CO)_8(NC_5H_5)(PPh_3)$ (**6**); 20% thermal ellipsoids are shown for the non-hydrogen atoms. Hydrogen atoms have arbitrary radii of 0.1 Å. Projections are shown (a) normal to and (b) oblique to the Ru_3 plane.

Our interest in this structure stemmed from locating the substitution site of the phosphine, which was found to ligate equatorially at the N-coordinated ruthenium, *trans* to a ruthenium–ruthenium bond. Day *et al.* [9] have discussed phosphine substitution on related imidoyl-ligated triosmium clusters. Although "preferential location of the phosphine under nitrogen *vs.* carbon... (is expected) on electronic grounds with the phosphine's greater donor ability balanced by the more electronegative nitrogen atom," their studies on $Os_3(\mu\text{-H})(\mu\text{-}\eta^2\text{-N=CCH}_2\text{CH}_2\text{CH}_2)(CO)_9(PPh_3)$ afforded a 4:1 isomeric mixture, with C ligation predominant over N ligation. In related studies, Adams and coworkers characterized $Os_3(\mu\text{-H})(\mu\text{-}\eta^2\text{-PhN=CH})(CO)_9[P(OCH_3)_3]$ [10] and $Os_3(\mu\text{-H})(\mu\text{-}\eta^2\text{-CF}_3\text{C=NH})(CO)_9(PMe_2Ph)$ [11]; in these cases, substitution occurred at the osmium atom bearing the imidoyl donor atom with the H substituent, *i.e.* the sterically less demanding site. For the pyrrolidyl and pyridyl clusters, site discrimination on steric grounds should not be important; the reasons for substitutional differences between these two systems are not clear, but our product is consistent with the probability that site specificity is driven by electronic considerations. Caution must be exercised in pursuing these arguments too far, however; the long Ru–CO distance *trans* to the imidoyl carbon atom suggests that this group also functions as a good acceptor. The phosphine coordination geometry itself is nor-

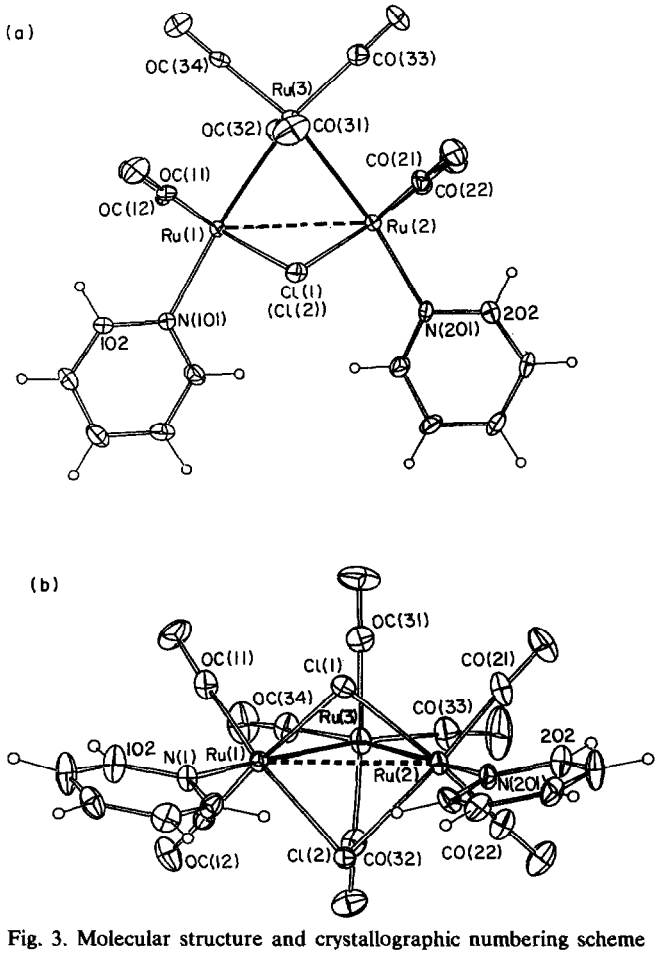

Fig. 3. Molecular structure and crystallographic numbering scheme for $Ru_3(\mu\text{-Cl})_2(CO)_8(NC_5H_5)_2$ (molecule 1) (**7**); 20% thermal ellipsoids are shown for the non-hydrogen atoms. Hydrogen atoms have arbitrary radii of 0.1 Å. Projections are shown (a) normal to and (b) oblique to the Ru_3 plane.

TABLE 4. Atomic coordinates and equivalent isotropic thermal parameters for $Ru_3(\mu\text{-Cl})_2(CO)_8(NC_5H_5)(PPh_3)$ (**6**)

Atom	*x*	*y*	*z*	U_{eq} (Å^2)
Ru(1)	0.29385 (4)	0.59436 (7)	0.25158 (9)	0.0388 (3)
Ru(2)	0.12893 (5)	0.72783 (8)	0.1329 (1)	0.0450 (3)
Ru(3)	0.26450 (5)	0.85618 (8)	0.0834 (1)	0.0491 (4)
Cl(1)	0.2005 (1)	0.5469 (2)	0.0843 (3)	0.046 (1)
Cl(2)	0.1760 (1)	0.6174 (2)	0.3911 (3)	0.049 (1)
C(11)	0.3727 (6)	0.592 (1)	0.121 (1)	0.048 (4)
O(11)	0.4207 (5)	0.5923 (8)	0.0396 (9)	0.078 (4)
C(12)	0.3593 (6)	0.650 (1)	0.364 (1)	0.055 (5)
O(12)	0.4036 (5)	0.6841 (9)	0.430 (1)	0.089 (4)
C(21)	0.1041 (6)	0.808 (1)	−0.065 (1)	0.057 (5)
O(21)	0.0873 (5)	0.8555 (8)	−0.188 (1)	0.086 (4)
C(22)	0.0848 (6)	0.864 (1)	0.176 (1)	0.061 (5)
O(22)	0.0543 (5)	0.9478 (9)	0.204 (1)	0.097 (5)
C(31)	0.2695 (6)	0.801 (1)	−0.099 (1)	0.059 (5)
O(31)	0.2767 (5)	0.7767 (9)	−0.204 (1)	0.086 (4)
C(32)	0.2518 (7)	0.876 (1)	0.280 (1)	0.065 (5)
O(32)	0.2451 (5)	0.8923 (8)	0.395 (1)	0.083 (4)
C(33)	0.2173 (7)	1.022 (1)	−0.013 (1)	0.071 (6)
O(33)	0.1912 (6)	1.1226 (9)	−0.067 (1)	0.105 (5)
C(34)	0.3684 (7)	0.897 (1)	0.072 (1)	0.062 (5)
O(34)	0.4304 (5)	0.922 (1)	0.064 (1)	0.101 (5)
P(1)	0.3093 (2)	0.3732 (3)	0.4099 (3)	0.041 (1)
C(111)	0.3346 (5)	0.3566 (9)	0.603 (1)	0.044 (4)
C(112)	0.3824 (7)	0.257 (1)	0.689 (1)	0.071 (6)
C(113)	0.4003 (8)	0.247 (1)	0.837 (1)	0.085 (6)
C(114)	0.3727 (8)	0.334 (1)	0.902 (1)	0.071 (6)
C(115)	0.3272 (7)	0.431 (1)	0.820 (1)	0.075 (6)
C(116)	0.3061 (6)	0.445 (1)	0.673 (1)	0.061 (5)
C(121)	0.3851 (6)	0.276 (1)	0.357 (1)	0.047 (4)
C(122)	0.3769 (7)	0.150 (1)	0.363 (1)	0.071 (6)
C(123)	0.437 (1)	0.078 (1)	0.331 (2)	0.100 (8)
C(124)	0.505 (1)	0.131 (2)	0.294 (2)	0.098 (8)
C(125)	0.5154 (7)	0.254 (2)	0.290 (1)	0.081 (7)
C(126)	0.4555 (7)	0.328 (1)	0.322 (1)	0.062 (5)
C(131)	0.2267 (6)	0.2810 (9)	0.427 (1)	0.047 (4)
C(132)	0.1838 (7)	0.243 (1)	0.557 (1)	0.071 (5)
C(133)	0.1205 (8)	0.175 (1)	0.564 (2)	0.079 (6)
C(134)	0.0986 (8)	0.139 (1)	0.443 (2)	0.094 (8)
C(135)	0.1388 (8)	0.179 (1)	0.310 (2)	0.077 (6)
C(136)	0.2015 (7)	0.248 (1)	0.301 (1)	0.059 (5)
N(1)	0.0298 (5)	0.6090 (8)	0.184 (1)	0.052 (4)
C(2)	−0.0377 (7)	0.658 (1)	0.120 (1)	0.074 (6)
C(3)	−0.1023 (6)	0.587 (1)	0.145 (1)	0.068 (5)
C(4)	−0.0984 (6)	0.465 (1)	0.238 (1)	0.068 (6)
C(5)	−0.0310 (7)	0.414 (1)	0.303 (2)	0.076 (6)
C(6)	0.0317 (6)	0.487 (1)	0.274 (1)	0.066 (5)

TABLE 5. Atomic coordinates and equivalent isotropic thermal parameters for $Ru_3(\mu\text{-}Cl)_2(CO)_8(NC_5H_5)_2$ (7)

Atom	x	y	z	U_{eq} (Å^2)
Molecule 1				
Ru(11)	0.83158 (9)	0.44618 (4)	0.77092 (7)	0.0320 (5)
Ru(12)	1.02961 (9)	0.37405 (4)	0.76524 (8)	0.0366 (5)
Ru(13)	0.98340 (9)	0.47431 (4)	0.69941 (8)	0.0411 (6)
C(111)	0.865 (1)	0.5076 (5)	0.832 (1)	0.048 (7)
O(111)	0.890 (1)	0.5460 (4)	0.8727 (8)	0.084 (7)
C(112)	0.709 (1)	0.4767 (5)	0.669 (1)	0.042 (7)
O(112)	0.6316 (9)	0.4972 (4)	0.6036 (7)	0.070 (6)
C(121)	1.189 (1)	0.3895 (6)	0.819 (1)	0.058 (8)
O(121)	1.2886 (9)	0.3991 (4)	0.8475 (8)	0.087 (7)
O(122)	1.042 (1)	0.3457 (4)	0.5919 (8)	0.084 (7)
C(122)	1.034 (1)	0.3557 (5)	0.656 (1)	0.056 (9)
C(131)	1.097 (1)	0.4922 (5)	0.831 (1)	0.057 (9)
O(131)	1.164 (1)	0.5049 (4)	0.9072 (8)	0.093 (7)
C(132)	0.857 (1)	0.4479 (5)	0.581 (1)	0.052 (8)
O(132)	0.782 (1)	0.4340 (4)	0.5102 (7)	0.076 (6)
C(133)	1.096 (1)	0.4766 (5)	0.654 (1)	0.066 (9)
O(133)	1.159 (1)	0.4761 (5)	0.623 (1)	0.13 (1)
C(134)	0.924 (1)	0.5426 (5)	0.664 (1)	0.051 (8)
O(134)	0.887 (1)	0.5818 (4)	0.640 (1)	0.097 (9)
Cl(11)	1.0038 (3)	0.4020 (1)	0.9016 (2)	0.043 (2)
Cl(12)	0.8087 (3)	0.3630 (1)	0.6890 (2)	0.038 (1)
N(1101)	0.7189 (9)	0.4175 (4)	0.8317 (7)	0.040 (5)
C(1102)	0.655 (1)	0.4489 (5)	0.852 (1)	0.064 (9)
C(1103)	0.583 (1)	0.4347 (7)	0.888 (1)	0.08 (1)
C(1104)	0.569 (1)	0.3841 (7)	0.901 (1)	0.065 (9)
C(1105)	0.634 (1)	0.3519 (5)	0.879 (1)	0.060 (9)
C(1106)	0.706 (1)	0.3689 (5)	0.846 (1)	0.049 (8)
N(1201)	1.0552 (9)	0.2971 (4)	0.8275 (7)	0.042 (5)
C(1202)	1.154 (1)	0.2693 (6)	0.848 (1)	0.059 (8)
C(1203)	1.174 (1)	0.2214 (6)	0.885 (1)	0.08 (1)
C(1204)	1.092 (1)	0.2004 (5)	0.907 (1)	0.057 (8)
C(1205)	0.992 (1)	0.2274 (5)	0.888 (1)	0.055 (8)
C(1206)	0.977 (1)	0.2746 (5)	0.848 (1)	0.050 (7)
Molecule 2				
Ru(21)	0.65413 (9)	0.14703 (4)	0.69556 (7)	0.0343 (5)
Ru(22)	0.44921 (9)	0.22050 (4)	0.68483 (7)	0.0332 (5)
Ru(23)	0.49037 (9)	0.12126 (4)	0.75631 (7)	0.0354 (5)
C(211)	0.777 (1)	0.1206 (5)	0.8041 (9)	0.038 (7)
O(211)	0.8565 (9)	0.1028 (4)	0.8712 (7)	0.072 (6)
C(212)	0.624 (1)	0.0845 (5)	0.642 (1)	0.049 (8)
O(212)	0.606 (1)	0.0443 (4)	0.6096 (8)	0.077 (7)
C(221)	0.431 (1)	0.2381 (5)	0.786 (1)	0.043 (7)
O(221)	0.4182 (9)	0.2491 (4)	0.8501 (7)	0.074 (6)
C(222)	0.291 (1)	0.2040 (5)	0.620 (1)	0.049 (8)
O(222)	0.1908 (9)	0.1949 (4)	0.5801 (8)	0.077 (6)
C(231)	0.602 (1)	0.1531 (5)	0.874 (1)	0.046 (8)
O(231)	0.6666 (9)	0.1715 (4)	0.9464 (7)	0.072 (6)
C(232)	0.384 (1)	0.0992 (5)	0.625 (1)	0.049 (7)
O(232)	0.322 (1)	0.0858 (4)	0.5500 (8)	0.077 (6)
C(233)	0.364 (1)	0.1208 (5)	0.786 (1)	0.052 (8)
O(233)	0.289 (1)	0.1217 (4)	0.8047 (9)	0.088 (8)
C(234)	0.550 (1)	0.0543 (6)	0.800 (1)	0.054 (8)
O(234)	0.583 (1)	0.0140 (4)	0.8245 (9)	0.088 (7)
Cl(21)	0.6698 (3)	0.2325 (1)	0.7680 (2)	0.038 (1)
Cl(22)	0.4852 (3)	0.1891 (1)	0.5562 (2)	0.042 (2)
N(2101)	0.7755 (8)	0.1740 (4)	0.6405 (7)	0.040 (5)
C(2102)	0.852 (1)	0.1426 (5)	0.636 (1)	0.058 (9)
C(2103)	0.932 (1)	0.1551 (7)	0.607 (1)	0.09 (1)
C(2104)	0.930 (1)	0.2039 (6)	0.579 (1)	0.065 (9)
C(2105)	0.853 (1)	0.2379 (5)	0.582 (1)	0.058 (8)
C(2106)	0.777 (1)	0.2220 (5)	0.615 (1)	0.050 (8)
N(2201)	0.4331 (8)	0.2999 (4)	0.6297 (7)	0.039 (5)
C(2202)	0.358 (1)	0.3321 (5)	0.639 (1)	0.059 (9)
C(2203)	0.348 (1)	0.3822 (6)	0.608 (1)	0.07 (1)
C(2204)	0.414 (1)	0.3995 (5)	0.570 (1)	0.058 (8)
C(2205)	0.491 (1)	0.3667 (5)	0.560 (1)	0.056 (7)
C(2206)	0.497 (1)	0.3179 (5)	0.592 (1)	0.047 (7)

mal and the Ru(1)–P(1) distance (2.379(2) Å) and intraphosphine lengths and angles are not unusual.

The products in bands 6–8 were all minor but were all characterized. That from band 6 was crystallized and identified as $Ru_3(\mu\text{-}Cl)_2(CO)_8(PPh_3)_2$ (**5**), obtained in earlier work from the pyrolysis of **1** [5]. The previously unreported ^{13}C NMR spectrum shows the expected signals due to the phenyl carbon atoms, together with a resonance at 209.8 ppm due to the fluxional carbonyl ligands. The products in bands 7 and 8 were crystallized and identified as $Ru_3(\mu\text{-}Cl)_2(CO)_8(NC_5H_5)(PPh_3)$ (**6**) and $Ru_3(\mu\text{-}Cl)_2(CO)_8(NC_5H_5)_2$ (**7**) respectively, related to **5** by sequential replacement of PPh_3 by pyridine. Compound **6** was identified by the usual spectroscopic means. The ^1H NMR spectrum contains signals due to the aromatic protons of the phenyl groups as a multiplet at 7.54–7.41 ppm. The pyridine signals appear at 8.38 (2H) ppm, 8.02 (1H) ppm and 7.30 (2H) ppm and are assigned to H2 and H6, to H4 and to H3 and H5 respectively of the pyridine ring. The ^{13}C NMR spectrum contains a signal at 208.7 ppm due to the fluxional coordinated carbonyl groups, and signals at 152.1 ppm, 133.0 ppm and 125.1 ppm assigned to C2 and C6, to C4 and to C3 and C5 respectively of the pyridine. The FAB mass spectrum does not contain a molecular ion; rather, at highest m/z there is a signal due to the loss of the pyridine ligand from the parent ion, a result which is consistent with the "lightly stabilizing" nature of this group observed in other cluster chemistry. Owing to the instability of **6**, it was not possible to obtain a satisfactory microanalysis. Difficulties were encountered in isolating compound **7** as a pure sample, despite repeated thin layer chromatography. The IR spectrum of **7** and a crystal for the X-ray studies were obtained by hand separation of crystals from a mixture with **5** and **6**. The IR spectrum shows four signals due to the carbonyl ligands instead of the five signals found in **6**, indicating a more symmetric cluster. Both **6** and **7** were subjected to single-crystal X-ray diffraction studies; the results are given below, together with a comparison with the

previously reported data for the related cluster **5** [12].

The solid state structures are shown in Fig. 2 (**6**) and Fig. 3 (**7**); crystallographic data are listed in Table 1, atomic coordinates in Table 4 (**6**) and Table 5 (**7**), selected bond lengths in Table 6, and selected bond angles in Table 7. Clusters **5**–**7** have V-shaped triruthenium cores, with the non-bonding vector (by Ru ··· Ru distance and EAN rule) spanned by two chloro ligands. The Ru–Ru bond distances (2.85 Å (average) (**5**), 2.82 Å (average) (**6**) and 2.80 Å (average) (**7**)) show a gradual contraction on replacement of PPh_3 by NC_5H_5. The non-bonding distances (3.25 Å (**5**), 3.23 Å (**6**) and 3.21 Å (average) (**7**)) in such clusters have been "related to the size of the bridgehead atoms... as a first approximation" [12]; maintaining the bridging group and varying other ligands in proceeding from **5** through **6** to **7** results in a similar contraction in the bonding distances, clearly showing that other factors can influence this distance. The Ru–CO distances fall clearly into two sets, with those to the terminal ruthenium atoms (1.82 Å (average) (**5**), 1.83 Å (average) (**6**) and 1.82 Å (average) (**7**)) significantly shorter than those to the bridging ruthenium atom (1.91 Å (average) (**5**), 1.93 Å (average) (**6**) and 1.92 Å (average (**7**)); in the case of **5**, this was attributed to a "*trans* shortening influence (of the) Cl atoms" [12].

TABLE 6. Selected bond lengths for $Ru_3(\mu\text{-}Cl)_2(CO)_8(PPh_3)_2$ (**5**) [a], $Ru_3(\mu\text{-}Cl)_2(CO)_8(NC_5H_5)(PPh_3)$ (**6**) [b] and $Ru_3(\mu\text{-}Cl)_2(CO)_8(NC_5H_5)_2$ (**7**) [b,c]

	Bond length (Å)		
	5	**6**	**7**
Ru(1)···Ru(2)	3.254 (1)	3.234 (1)	3.209 (2), 3.200 (2)
Ru(1)–Ru(3)	2.845 (1)	2.843 (2)	2.801 (2), 2.798 (2)
Ru(2)–Ru(3)	2.860 (1)	2.803 (1)	2.797 (2), 2.797 (2)
Ru(1)–Cl(1)	2.461 (2)	2.467 (3)	2.463 (3), 2.494 (3)
Ru(1)–Cl(2)	2.470 (2)	2.485 (3)	2.496 (3), 2.479 (3)
Ru(2)–Cl(1)	2.464 (3)	2.465 (3)	2.476 (4), 2.485 (3)
Ru(2)–Cl(2)	2.472 (2)	2.465 (3)	2.491 (4), 2.464 (4)
Cl(1)...Cl(2)	3.194 (4)	3.214 (4)	3.245 (4), 3.242 (4)
Ru(1)–N, *P*	*2.402 (2)*	*2.425 (3)*	2.23 (1), 2.25 (1)
Ru(2)–N, *P*	*2.432 (3)*	2.20 (1)	2.21 (1), 2.24 (1)
Ru(1)–C(11)	1.823 (9)	1.85 (1)	1.83 (1), 1.81 (1)
Ru(1)–C(12)	1.809 (12)	1.82 (1)	1.80 (1), 1.81 (1)
Ru(2)–C(21)	1.817 (11)	1.83 (1)	1.83 (2), 1.81 (2)
Ru(2)–C(22)	1.815 (11)	1.81 (1)	1.85 (2), 1.82 (1)
Ru(3)–C(31)	1.919 (11)	1.97 (1)	1.94 (1), 1.91 (1)
Ru(3)–C(32)	1.923 (12)	1.92 (1)	1.92 (1), 1.94 (1)
Ru(3)–C(33)	1.886 (11)	1.92 (1)	1.91 (2), 1.90 (2)
Ru(3)–C(34)	1.909 (11)	1.90 (1)	1.93 (1), 1.91 (1)

[a] Reference 12; atom labelling as per **6** and **7** in this work.
[b] This work.
[c] The two entries are for two molecules in the asymmetric unit.

TABLE 7. Selected bond angles for $Ru_3(\mu\text{-}Cl)_2(CO)_8(PPh_3)_2$ (**5**) [a], $Ru_3(\mu\text{-}Cl)_2(CO)_8(PPh_3)(NC_5H_5)$ (**6**) [b] and $Ru_3(\mu\text{-}Cl)_2(CO)_8(NC_5H_5)_2$ (**7**) [b,c]

	Bond angle (°)		
	5	**6**	**7**
Ru(1)–Ru(3)–Ru(2)	69.55 (3)	69.90 (4)	69.96 (5), 69.76 (5)
Ru(1)···Ru(2)–Ru(3)	55.01 (2)	55.63 (4)	55.09 (4), 55.13 (4)
Ru(3)–Ru(1)···Ru(2)	55.42 (2)	54.57 (3)	54.95 (5), 55.11 (5)
Cl(1)–Ru(1)–Cl(2)	80.65 (9)	80.9 (1)	81.7 (1), 81.4 (1)
Cl(1)–Ru(2)–Cl(2)	80.54 (8)	81.4 (1)	81.6 (1), 81.8 (1)
Ru(1)–Cl(1)–Ru(2)	82.67 (8)	82.0 (1)	81.1 (1), 80.0 (1)
Ru(1)–Cl(2)–Ru(2)	82.35 (6)	81.59 (8)	80.1 (1), 80.7 (1)
N, *P*–Ru(1)···Ru(2)	*126.05 (5)*	*121.93 (7)*	120.2 (3), 119.8 (3)
N, *P*–Ru(1)–Ru(3)	*178.36 (6)*	*174.73 (8)*	175.1 (3), 174.8 (2)
N, *P*–Ru(2)···Ru(1)	*122.46 (6)*	118.4 (2)	118.3 (4), 120.0 (3)
N, *P*–Ru(2)–Ru(3)	*176.57 (7)*	174.0 (2)	173.0 (4), 174.9 (3)
C(11)–Ru(1)–C(12)	91.5 (5)	88.1 (5)	87.9 (5), 89.4 (5)
C(21)–Ru(2)–C(22)	89.7 (5)	88.1 (5)	87.3 (8), 88.2 (7)
C(31)–Ru(3)–C(32)	169.5 (4)	168.4 (5)	168.1 (8), 169.1 (7)
C(33)–Ru(3)–C(34)	101.1 (5)	100.4 (5)	96.8 (7), 98.0 (7)

[a] Reference 12; atom labelling as per **6** and **7** in this work.
[b] This work.
[c] The two entries are for two molecules in the asymmetric unit.

Triruthenium clusters containing unsupported σ-bound pyridine ligands are extremely rare; to our knowledge, the only such complex structurally characterized previously was $Ru_3(\mu\text{-}H)(\mu\text{-}CNMe_2)(CO)_9(NC_5H_5)$ (**8**), in which the pyridine occupies a "semiaxial" site, adjacent to the bridging hydride [13]; by contrast, the pyridines in **6** and **7** are equatorially ligated. The Ru–N distance in **8** was reported as 2.250 (5) Å and those in **6** and **7** are 2.20 (3) Å and 2.24(1) Å (average) respectively. These are the largest Ru–N distances thus far observed in ruthenium carbonyl clusters with nitrogen ligands [2]; very long Ru–N separations revealed by crystallographic characterization of **6**–**8** support the view that pyridine's role is a "lightly stabilizing" ligand in trimetallic carbonyl cluster chemistry.

σ-bound pyridine is the supposed intermediate in cluster-activated conversion of free pyridine into ligated pyridyl and is therefore of importance in hydrotreating modelling. The low yields of **6** and **7** have precluded an investigation of their chemistry, but the available data (the observation of $[M\text{–pyridine}]^+$ rather than molecular ion in the MS, and the extremely long Ru–N distances revealed by the X-ray structural studies) suggest that loss of pyridine rather than orthometallation is likely in this system.

Conventional routes into mixed-metal clusters incorporating (triphenylphosphine)gold involve (a) formation of a cluster anion and then reaction with $AuX(PPh_3)$ [14] or (b) reaction of a cluster hydride with $AuMe(PPh_3)$, with concomitant reductive elimina-

tion of methane [15]. Deprotonation of **1** by K-Selectride or proton sponge to generate a cluster anion, followed by reaction with $[Au(PPh_3)]^+$ afforded a mixture of products in both cases, of which **4** was identified as the major constituent. Similarly, direct reaction between **1** and $AuMe(PPh_3)$ gave a large number of products, with **4** in highest yield.

3. Conclusion

Attempts to make mixed-metal aurotriruthenium clusters containing pyridyl or pyridine ligands by a variety of routes were unsuccessful; however, the reactions did proceed by complex pathways to gave mixtures of products involving site-specific phosphine substitution on a (pyridyl)triruthenium cluster and, in one case, to a unique series of dichloro-bridged triruthenium clusters related by successive replacement of PPh_3 by NC_5H_5.

4. Experimental details

$Ru_3(\mu\text{-}AuPPh_3)(\mu\text{-}Cl)(CO)_{10}$ (**1**) was synthesized from $Ru_3(CO)_{12}$ as previously described [5]. K-selectride and proton sponge were purchased from Aldrich. Pyridine was obtained from May and Baker and was used without further purification. Chloro(triphenylphosphine)gold(I) was synthesized from chloroauric acid [16] and converted into methyl(triphenylphosphine)gold(I) by the published procedure [17]. THF was distilled from Na–benzophenone under an inert atmosphere prior to use. The reactions were carried out by use of standard Schlenk techniques [18] under dry argon or nitrogen, although subsequent work-up was carried out without precautions to exclude air. Thin layer chromatography was on glass plates (20 cm × 20 cm) coated with Merck GF_{254} silica gel (0.5 mm).

IR spectra were recorded using a Perkin–Elmer model 1725 Fourier transform spectrophotometer with CaF_2 optics. NMR spectra were recorded on a Bruker AM300 spectrometer, the ^1H spectra at 300.13 MHz, and the ^{13}C spectra at 75.47 MHz, using approximately 0.04 M $Cr(acac)_3$ as the relaxation agent and a recycle delay of 0.5 s. FAB mass spectra were recorded using a VG ZAB 2HF instrument (exciting gas, Ar; source pressure, 10^{-6} mbar; FAB gun voltage, 7.5 kV; current, 1 mA; accelerating potential, 8 kV) at the University of Adelaide. The matrix was 3-nitrobenzyl alcohol. Peaks were recorded as m/z. The elemental analysis was by Dr O.b. Shawkataly at the Universiti Sains Malaysia, Penang, Malaysia.

4.1. Reaction between $Ru_3(\mu\text{-}AuPPh_3)(\mu\text{-}Cl)(CO)_{10}$ and pyridine

Pyridine (33 mg, 0.42 mmol) was added to a solution of $Ru_3(\mu\text{-}AuPPh_3)(\mu\text{-}Cl)(CO)_{10}$ (253 mg, 0.24 mmol) in THF (40 ml) and the mixture heated under reflux for 40 min. The resulting dark-yellow–brown solution was taken to dryness and subjected to repeated thin layer chromatography, with 5–15% acetone in petrol as eluent, to give eight bands, from which the following products were identified. The products isolated from bands 1 and 2 were crystallized from saturated hexane solutions at −20°C to give yellow crystals of $Ru_3(\mu\text{-}H)(\mu\text{-}NC_5H_4)(CO)_{10}$ (**2**) [4] (yield, 9 mg (6%)) and red crystals of $Ru_3(CO)_{10}(PPh_3)_2$ (**3**) [6] (yield, 6 mg (2%)) respectively. Those from bands 4, 6, 7 and 8 were crystallized from CH_2Cl_2–hexane at −20°C to yield orange crystals of $Ru_3(\mu\text{-}H)(\mu\text{-}NC_5H_4)(CO)_9(PPh_3)$ (**4**) (yield, 17 mg (8%)) and $Ru_3(\mu\text{-}Cl)_2(CO)_8(PPh_3)_2$ (**5**) [5,12] (yield, 10 mg (4%)) and yellow crystals of $Ru_3(\mu\text{-}Cl)_2(CO)_8(NC_5H_5)(PPh_3)$ (**6**) (yield, 4 mg (2%)) and $Ru_3(\mu\text{-}Cl)_2(CO)_8(NC_5H_5)_2$ (**7**) (less than 1 mg) respectively. Bands 3 and 5 were very minor and their contents as yet unidentified.

The known complexes were identified by comparison of their IR and NMR data with the values in the literature.

4.2. Analytical data

4: Anal. Found: C, 43.47; H, 2.37; N, 1.31, $C_{32}H_{20}NO_9PRu_3$ calc.: C, 42.86; H, 2.25; N, 1.56% m/z. Found: 869 $[M-CO]^+$. $C_{32}H_{20}NO_9PRu_3$ calc.: 897 (M^+) IR (cyclohexane): ν(CO) 2083m, 2043s, 2015s, 2010m(sh), 2002m, 1991w, 1984w, 1974w, 1954w cm^{-1}. ^1H NMR (CD_2Cl_2): 7.45–7.31 (m, 16H, Ph + H6 of pyridyl); pyridyl: 7.25 (m, 1H, H3); 7.00 (m, 1H, H4); 6.24 (m, 1H, H5); −14.08 (d, J(HP) = 9 Hz, 1H, Ru–H) ppm. ^{13}C NMR (CD_2Cl_2) CO: 191.8; pyridyl: 179.6 (C2); 153.9 (C6); 138.5 (C3); 132.8 (C4); 120.6 (C5) phosphine: 134.1 (d, ^1J(CP) = 40 Hz, C1); 133.6 (d, ^2J(CP) = 11 Hz, C2, 6); 130.4 (s, C4); 128.9 (d, ^3J(CP) = 10 Hz, C3, 5) ppm.

5: ^{13}C NMR (CD_2Cl_2) CO: 209.8; phosphine: 134.3 (d, ^2J(CP) = 11 Hz, C2, 6); 132.1 (d, ^1J(CP) = 38 Hz, C1); 131.2 (s, C4); 129.3 (d, ^3J(CP) = 9 Hz, C3, 5) ppm.

6: m/z. Found: 861 ($M^+ - NC_5H_5$) $C_{31}H_{20}Cl_2NO_8PRu_3$ calc.: 940 (M^+) IR (cyclohexane): ν(CO) 2085m, 2019s, 2005w, 1958w, 1954w cm^{-1}. ^1H NMR (d_6-acetone): 7.54–7.41 (m, 15H, Ph) pyridyl: 8.38 (m, 2H, H2, 6); 8.02 (m, 1H, H4); 7.30 (m, 2H, H3, 5) ppm. ^{13}C NMR (d_6-acetone) CO: 208.69; pyridine: 152.1 (C2, 6); 133.0 (C3, 5); 125.1 (C4) ppm.

7: IR (CH_2Cl_2): ν(CO) 2089m, 2023sh, 2013s, 1940m cm^{-1}.

4.3. Reaction between $Ru_3(\mu\text{-}H)(\mu\text{-}NC_5H_4)(CO)_{10}$ and triphenylphosphine

Triphenylphosphine (12 mg, 0.045 mmol) was added to a solution of $Ru_3(\mu\text{-}H)(\mu\text{-}NC_5H_4)(CO)_{10}$ (30 mg, 0.045 mmol) in THF (5 ml) and the mixture stirred for 30 min. Chromatographic work-up with petrol as eluent afforded two bands. The content of the first band was identified as unchanged $Ru_3(\mu\text{-}H)(\mu\text{-}NC_5H_4)(CO)_{10}$ by IR spectroscopy. The product isolated from the second band was recrystallized from hexane at −20°C to give orange crystals identified as $Ru_3(\mu\text{-}H)(\mu\text{-}NC_5H_4)(CO)_9(PPh_3)$ (**4**) (yield, 32 mg (81%)).

4.4. Reactions between $Ru_3(\mu\text{-}H)(\mu\text{-}NC_5H_4)(CO)_{10}$ and (triphenylphosphine)gold(I) complexes

4.4.1. K-Selectride / (triphenylphosphine)gold(I)$^+$

K-selectride (0.22 ml of a 1 M solution in THF) was added dropwise to a stirred solution of $Ru_3(\mu\text{-}H)(\mu\text{-}NC_5H_4)(CO)_{10}$ (70 mg, 0.11 mmol) in THF (15 ml) at −63°C. A mixture of $AuCl(PPh_3)$ (54 mg, 0.11 mmol) and $Ag[BF_4]$ (21 mg, 0.11 mmol) in THF (10 ml) was stirred for 15 min and then added through a Schlenk filter to the solution of the Ru complex. The resulting dark-red solution was allowed to come to room temperature and stirred for 90 min. Chromatography with 20% acetone in petrol as eluent afforded several bands, of which band 1 was shown to contain unchanged $Ru_3(\mu\text{-}H)(\mu\text{-}NC_5H_4)(CO)_{10}$ by IR. The product from band 2 was recrystallized from CH_2Cl_2–hexane to yield orange crystals of $Ru_3(\mu\text{-}H)(\mu\text{-}NC_5H_4)(CO)_9(PPh_3)$ (**4**) (yield, 16 mg (16%)).

4.4.2. Proton sponge–(triphenylphosphine)gold(I)$^+$

A solution of $[Au(PPh_3)]^+$ prepared as above ($AuCl(PPh_3)$ (27 mg, 0.054 mmol) and $Ag[BF_4]$ (11 mg, 0.054 mmol) in THF (15 ml)) was added dropwise to a stirred solution of $Ru_3(\mu\text{-}H)(\mu\text{-}NC_5H_4)(CO)_{10}$ (30 mg, 0.045 mmol) and proton sponge (10 mg, 0.045 mmol) in THF (15 ml). The mixture was passed through a Schlenk filter to remove the resulting brown precipitate and the orange solution stirred for 6 days, after which no starting material could be observed by IR spectroscopy. Chromatographic work-up with 25% CH_2Cl_2 in petrol as eluent gave a multitude of bands, from which the major product was identified as $Ru_3(\mu\text{-}H)(\mu\text{-}NC_5H_4)(CO)_9(PPh_3)$ (**4**) (yield 4 mg (10%)) by IR and FAB MS.

4.4.3. Methyl(triphenylphosphine)gold(I)

A solution of $Ru_3(\mu\text{-}H)(\mu\text{-}NC_5H_4)(CO)_{10}$ (40 mg, 0.060 mmol) and $AuMe(PPh_3)$ (34 mg, 0.072 mmol) in THF (20 mL) was stirred for 16 h during which IR monitoring revealed no evidence of reaction. Refluxing for 90 min followed by chromatographic work-up with 15% acetone in petrol as eluent afforded a multitude of bands, from which only $Ru_3(\mu\text{-}H)(\mu\text{-}NC_5H_4)(CO)_9(PPh_3)$ (**4**) (yield, 15 mg (28%)) was identified by IR spectroscopy.

4.5. Structure determinations

Unique diffractometer data sets (2θ–θ scan mode; monochromatic Mo Kα radiation, $\lambda = 0.7107_3$ Å) were measured within the specified $2\theta_{max}$ limit at about 295 K, yielding N independent reflections; N_o of these with $I > 3\sigma(I)$ were considered observed and used in the full-matrix least-squares refinements after gaussian absorption correction. Anisotropic thermal parameters were refined for the non-hydrogen atoms; $(x, y, z, U_{iso})_H$ were included fixed at estimated values. Conventional residuals R and R_w on $|F|$ are quoted at convergence; statistical weights, derivative of $\sigma^2(I) = \sigma^2(I_{diff}) + 0.0004\sigma^4(I_{diff})$ were used. Neutral atom complex scattering factors were employed; computation used the XTAL 3.0 program system implemented by Hall and Stewart [19]. Pertinent results are given in the figures and tables.

4.6. Abnormal features and variations in procedure

The cluster hydride of **4** was located from difference map considerations and refined in (x, y, z, U_{iso}).

Tables of thermal parameters and hydrogen atom coordinates and complete lists of bond lengths and angles have been deposited at the Cambridge Crystallographic Data Centre.

Acknowledgments

We thank the Australian Research Council for support of this work, and Dr. C. Adams for the FAB mass spectra. We also thank Johnson–Matthey Technology Centre for a generous loan of $RuCl_3 \cdot xH_2O$. M.P.C. holds a University of New England Postgraduate Research Award.

References

1 M.P. Cifuentes, M.G. Humphrey, B.W. Skelton and A.H. White, *J. Organomet. Chem., 458* (1993) 211.
2 M.I. Bruce, M.P. Cifuentes and M.G. Humphrey, *Polyhedron, 10* (1991) 227.
3 J.R. Katzer and R. Sivasubramanian, *Catal. Rev. Sci. Eng., 25* (1983) 459.

4 M.I. Bruce, M.G. Humphrey, M.R. Snow, E.R.T. Tiekink and R.C. Wallis, *J. Organomet. Chem., 314* (1986) 311.
5 G. Lavigne, F. Papageorgiou and J.-J. Bonnet, *Inorg. Chem., 23* (1984) 609.
6 M.I. Bruce, J.G. Matisons and B.K. Nicholson, *J. Organomet. Chem., 247* (1983) 321.
7 G.A. Foulds, B.F.G. Johnson and J. Lewis, *J. Organomet. Chem., 296* (1985) 147.
8 C.E. Kampe and H.D. Kaesz, *Inorg. Chem., 23* (1984) 4646.
9 M. Day, D. Espitia, K.I. Hardcastle, S.E. Kabir, E. Rosenberg, R. Gobetto, L. Milone and D. Osella, *Organometallics, 10* (1991) 3550.
10 R.D. Adams and N.M. Golembeski, *J. Am. Chem. Soc., 101* (1979) 2579.
11 R.D. Adams, D.A. Katahira and L.W. Wang, *J. Organomet. Chem., 219* (1981) 85.
12 J.-J. Bonnet, G. Lavigne and F. Papageorgiou, *J. Crystallogr. Spectrosc. Res., 16* (1986) 475.
13 M.R. Churchill, J.C. Fettinger and J.B. Keister, *Organometallics, 4* (1985) 1867.
14 B.F.G. Johnson, D.A. Kaner, J. Lewis, P.R. Raithby and M.A. Taylor, *Polyhedron, 1* (1982) 105.
15 L.J. Farrugia, J.A.K. Howard, P. Mitrprachachon, J.L. Spencer, F.G.A. Stone and P. Woodward, *J. Chem. Soc. Chem. Commun.*, (1978) 260.
16 M.I. Bruce, B.K. Nicholson and O.b. Shawkataly, *Inorg. Synth., 26* (1989) 325.
17 H. Schmidbaur and A. Shiotani, *Chem. Ber., 104* (1971) 2821.
18 D.F. Shriver and M.A. Drezdzon, *The Manipulation of Air Sensitive Compounds*, Wiley, New York, 1986.
19 S.R. Hall and J.M. Stewart (eds.), *The XTAL 3.0 Reference Manual*, Universities of Western Australia and Maryland, 1990.